Offprint

of

Chinese Science Bulletin

www.scichina.com

Chinese Science Bulletin (Semimonthly, ISSN 1001-6538). 16 Donghuangchenggen North Street, Beijing 100717, China. Edited by the Editorial Committee of *Chinese Science Bulletin*, Tel: 86-10-64019820; Fax: 86-10-64031816; E-mail: csb@scichina.com. Distributed (China mainland) by SCP; E-mail: marketing@scichina.com

Guide to Authors

Chinese Science Bulletin is a comprehensive academic journal cosponsored by the Chinese Academy of Sciences and the National Natural Science Foundation of China. Its primary mission is to encourage communication of the novel and important research results in various fields of natural sciences. The contributions are required to be readable and have immediate and far-reaching implications to a broader audience.

Chinese Science Bulletin is cited in CA, EI, JICST, and some products of ISI, including Science Citation Index (SCI-CDE), SCI Search, Current Contents (PC&E), and Research Alert.

Chinese Science Bulletin is published twice monthly by Science in China Press.

1. Contributions published in *Chinese Science Bulletin*
   - **Views & News:** Introduce and comment on the research highlights published in *Chinese Science Bulletin* and other international journals and outstanding work awarded the national prizes (1800 words).
   - **Progress:** Introduce and comment on the substantial advance and its importance in the fast-developing areas (3600 words).
   - **Review:** Summarize the representative progress in core scientific disciplines, comment on the research status, and make suggestions for the future work (10,000 words, with a 600-word abstract).
   - **Frontiers:** Comment on excitement and existing problems of core fields, and offer suggestions for the future research. The contributions are usually solicited by editor's invitation.
   - **Articles:** Originally report the innovative and valuable findings in natural sciences (9000 words, with a 300-word abstract).
   - **Brief Communication:** Briefly report the novel and innovative findings in natural sciences (1800 words). The accepted contributions will be scheduled for publication within one month.
   - **Forum:** Comment on the important academic issues, administration policies and state scientific programmes, and give views about the theoretical problems such as the relation between scientific development and social evolution (6000 words, with a 200-word abstract).
   - **Correspondence:** Discuss and make reply to the contributions published in *Chinese Science Bulletin*, or introduce and comment on a controversial issue of general interest (4000 words).
   - **Trend:** Report weighty scientific news, information, and academic affairs, as well as the significant international conferences held in China (800 words).
   - **Books:** Introduce and comment on quality monographs of natural sciences (800 words).
2. Contributions are required of a concise, focused account of the findings and reliable essential data. They should be well organized and written clearly and simply, avoiding exhaustive tables and figures. Authors are advised to use internationally agreed nomenclature, express all measurements in SI units, and quote all the relevant references.
3. To guarantee the regular peer review, authors should supply the editors with a copy of the manuscript on disk (in word or PDF format) together with 2 typescript copies. Submission should be accompanied by the following materials and information: (i) statements that contributions have not been submitted simultaneously to other journals, in whole or in part; (ii) clarification of discipline and intended column; (iii) corresponding information, including post address, postcode, telephone and fax numbers, and email address; and (iv) suggestions for three to five suitable independent referees and the individuals to be excluded, while telling why. Since the OFC of each issue is designed based on the content of contributions, full colour illustrations or photographs are always welcome.
4. The final decision to accept a contribution for publication will be made by the editorial committee of this journal. If the authors do not receive decision letter after two months, they can submit the contributions for publication elsewhere, except an agreement has been made in advance. Authors are usually informed timely if the contribution is not considered, but their manuscripts will not be returned, except for the photographic material asked to be sent back.
5. Once the contribution is accepted, authors will be informed to provide the revised manuscript and its English version within 15 days. Poor English expression will be rejected. Authors of one accepted contribution will be presented one copy sample and 30 copies of reprints.

Contributions should be sent to: Chinese Science Bulletin, Science in China Press, 16 Donghuangchenggen North Street, Beijing 100717, China Tel: +86 10 64034134; Fax: +86 10 64016350 or 64031816;
Email: csb@scichina.com; Website: www.scichina.com

Advertisements for recruitment and products are welcome.

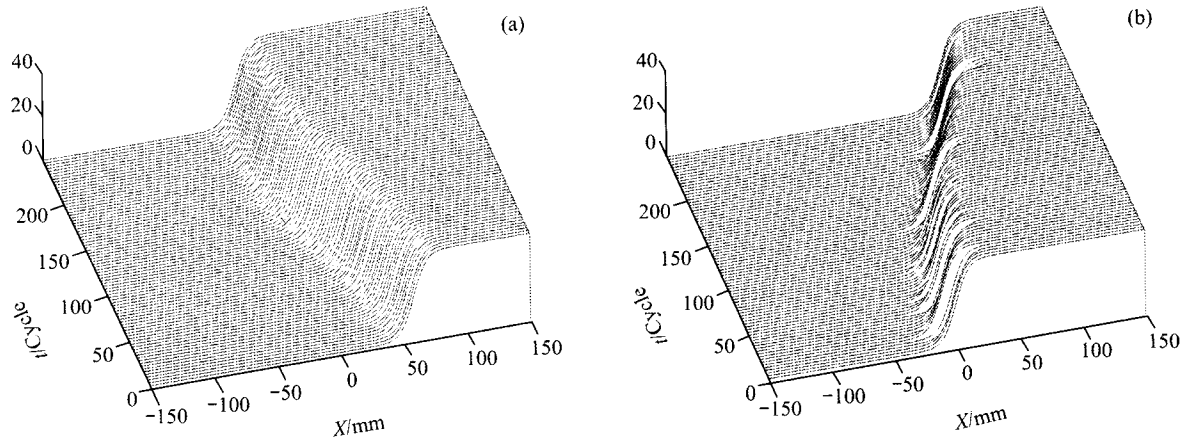

Fig. 4. Evolution of the interactions between impurities and a kink. (a) Shallow-impurity attracts the kink (Δd=−2 mm); (b) deep-impurity repels the kink (Δd=2 mm).

hence closer to the driving frequency. So energy is absorbed most at the shallow-impurity and is likely to become the swing center, which finally leads to the attraction on the breather. A deep-impurity absorbs energy least and is likely to become a still center, thus repels the breather. The kink, however, swings least at its center, so impurities that absorb less energy are more likely to become the center. To form a stable kink, one should drive the system a little bit higher (high-frequency driving) than the double parametric resonance frequency, so the shallow-impurity, farther from the resonance, is more suitable to become the kink center. In this case, shallow-impurity attracts the kink and the deep-impurity repels the kink, as the same in the breather case.

We have tried many different impurity intensities in our experiments and found that an over intensified impurity will turn over the interaction even the intensity polarity is not changed. For example, when the absolute intensity $|\Delta d|$ of the shallow-impurity become too high (Δd<−6 mm), it no longer attracts breathers and even repels them. An over intensified deep-impurity (Δd>3 mm) would also attract the kinks. These phenomena can be easily understood from the view of frequency matching and energy absorption[10].

4 Summary

We have observed the interaction between hydrodynamic solitons and impurities which are located on the bottom of the trough subject to vertical vibrations. Shallow-impurities attract the breather and kink and deep-impurities repel them. These observations meet the theoretical predictions in ref. [10]. The experimental results of the continuous system consist with previous theoretical and experimental works in discrete systems, which proves that the rules of interactions between solitons and impurities are universal.

Acknowledgements This work was jointly supported by the National Natural Science Foundation of China (Grant No. 10374050), the Special Funds for Major State Based Research Projects and the Trans-Century Training Program Foundation for the Talents by the State Education Commission.

References

1. Hennig, D., Tsironis, G. P., Wave transmission in nonlinear lattices, Phys. Rep., 1999, 307: 333—432.
2. Strogatz, S. H., Ordering chaos with disorder, Nature, 1995, 378: 444.
3. Braiman, Y., Lindner, J. F., Ditto, W. L., Taming spatiotemporal chaos with disorder, Nature, 1995, 378: 465.
4. Braun, O. M., Kivshar, Y. S., Nonlinear dynamics of the Frenkel-Kontorova model, Phys. Rep., 1998, 306(1): 1—108.
5. Braun, O., Paliy, M., Hu, B., "Fuse Safety Device" on an atomic scale, Phys. Rev. Lett., 1999, 83: 5206—5209.
6. Michel, R., Waves Called Solitons, Beijing: World Publishing Corporation, 1999, 137—166.
7. Scharf, R., Bishop, A. R., Properties of the nonlinear Schrödinger-equation on a lattice, Phys. Rev. A, 1991, 43(12): 6535—6544.
8. Gavrielides, A., Kottos, T., Kovanis, V. et al., Spatiotemporal organization of coupled nonlinear pendula trough impurities, Phys. Rev. E, 1998, 58: 5529—5534.
9. Alexeeva, N. V., Barashenkov, I. V., Tsironis, G. P., Impurity-induced stabilization of solitons in arrays of parametrically driven nonlinear oscillators, Phys. Rev. Lett., 2000, 84: 3053—3056.
10. Chen, W. Z., Hu, B., Zhong, H., Interactions between impurities and nonlinear waves in a driven nonlinear pendulum chain, Phys. Rev. B, 2002, 65: 134302—134309.
11. Miles, J. W., Parametrically excited solitary waves, Journal of Fluid Mech., 1984, 148: 451—460.
12. Wu, J., Keolian, R., Rudnick, I., Observation of a nonpropagating hydrodynamic soliton, Phys. Rev. Lett., 1984, 52: 1421—1424.
13. Denardo, B., Wright, W., Putterman, S., Observation of a kink soliton on the surface of a liquid, Phys. Rev. Lett., 1990, 64: 1518—1521.
14. Chen, W., Zhu, Y., Lu, L., Observations of impurity-soliton interactions in driven Frenkel-Kontorovachains, Phys. Rev. B, 2003, 67: 184301-1—184301-6.
15. Yan, J., Zhou, C., You, J., Nonpropagating soliton and kink soliton in a mildly sloping channel, Phys. Fluid A, 1992, 4(4): 690—694.

(Received January 30, 2004; accepted March 22, 2004)

Chinese Science Bulletin 2004 Vol. 49 No. 13 1342—1347

Direct observation of the clockwise light-driven rotation of F_oF_1-ATP synthase complex

CUI Yuanbo[1,2], ZHANG Yinghao[1,2], YUE Jiachang[1] & JIANG Peidong[1]

1. The National Laboratory of Biomacromolecules, Institute of Biophysics, Chinese Academy of Sciences, Beijing 100101, China;
2. The Graduate School of Chinese Academy of Sciences, Beijing 100039, China

Correspondence should be addressed to Yue Jiachang (e-mail: yuejc@sun5.ibp.ac.cn)

Abstract **The purified thermophilic bacterium PS3 $F_1\beta_{10\times His\text{-}tag}$ is inserted into the F_oF_1-ATP synthases of chromatophores isolated from photosynthetic bacteria *Rhodospirillum rubrum*. The studies of biochemical properties of the hybrid chromatophores show that they have both protons-driving capability and photophosphorylation. The fluorescent actin filaments, as a marker of its orientation by video-microscopic experiment, are connected via Maleimido-C_3-NTA to the reconstituted $\beta_{10\times His\text{-}tag}$ of F_oF_1-ATP synthases. The clockwise rotation of F_oF_1-ATP synthases driven by light is observed directly when viewed from the F_o side to F_1. This system should be valuable for further studying the coupling property of F_oF_1-ATP synthase.**

Keywords: photosynthetic bacteria chromatophores, F_oF_1-ATP synthase, molecular motor, light-driven, clockwise rotation.

DOI: 10.1360/04wc0009

The F_oF_1-ATP synthase, found in the inner membranes of mitochondria and chloroplasts and bacterial plasma, is involved in oxidative phosphorylation and photophosphorylation catalyzing the ATP synthesis from ADP and Pi. This enzyme in *E. coli* consists of two separate portions, F_1 and F_o. F_1 has a subunit composition of $\alpha_3\beta_3\gamma\delta\varepsilon$, and F_o has a subunit composition of ab_2c_n. The ATP synthesis takes place at the three β subunits of F_1[1—4].

It is well known that the ATP synthase is the smallest molecular motor in the world. In the single immobilized F_1 sub-complexes, subunit rotation during ATP hydrolysis has been demonstrated by Yoshida and his colleagues using a fluorescent actin filament connected to the γ subunit as a marker of its orientation by video-microscopic experiment in 1997[5]. Since then, many groups have observed its counterclockwise rotation during ATP hydrolysis when viewed from the F_o side to F_1[6—10]. In order to study the rotation of γ subunit during ATP synthesis, F_oF_1 sector purified with detergent-solubilized, and reconstituted into proteoliposomes, must be used. But both methods have technical limitations and difficulties. So the study of the rotation of γ subunit of F_oF_1-ATP synthase during ATP synthesis has become a very important issue.

Although the theory of proton-driven rotation of F_oF_1-ATP synthase in membrane holds true, direct observation of proton-driven rotation in the membrane by using the lipid bilayer membrane is a challenge. In this paper, using hybrid chromatophores, the clockwise rotation of F_oF_1-ATP synthase driven by light is observed directly when viewed from the F_o side to F_1.

1 Materials and methods

(i) Materials and reagents. Photosynthetic bacteria *Rhodospirillum rubrum* strain was presented by Prof. Zhang Xujia in our lab. Engineered F_1-ATPase (α, β and γ) was a gift from Dr. C. Montemagno[11]: the F_1-ATPase coding sequence was isolated from thermophilic bacterium, *Bacillus* PS3, and site-directed mutations of αCys193Ser and γSer107Cys were introduced and a ten histidine (His) tag was inserted immediately downstream of the β initiation codon. The mutated construct, pGEM-MH, was then cloned into the expression plasmid pQE-30, and the expression plasmid pQE-MH was inserted into *E. coli* JM103Δ(*uncB-uncD*) in which a majority of F_1-ATPase genes have been eliminated. The reagents, Pyruvate kinase, phosphoenolpyruvate, L-lactic dehydrogenase, Dicyclohexylcarbodiimide (DCCD), efrapeptin, Oligomycin, ATP, ADP, NADH, FITC and Glucose were all purchased from Sigma. Isoprophylthio-β-D-galactoside was commercially available from Bebco. ATP yields were determined by luciferin/luciferase kits purchased from LKB. Maleimido-C_3-NTA was purchased from Dojindo (Japan). Other chemicals were local products of analytical purity.

(ii) Preparation of hybrid system. Thermophilic bacterium, *Bacillus* PS3$\beta_{10\times His\text{-}tag}$ subunit ($TF_1\beta$) was expressed and purified as described in ref. [11] in which the JM103 strain expressing F_1-ATPase$\alpha_3(\beta_{10\times His\text{-}tag})_3\gamma$ was cultured in 2×YT medium (Amp^+) for 3—4 h at 37℃. When the A_{660} was 0.6—0.8, the expression of the F_1-ATPase was induced by adding 1 mmol/L isoprophylthio-β-D-galactoside for 3 h. Cells were harvested by centrifuging for 15 min at 4000×*g* and cell extracts were prepared using lysozyme (1 mg/mL)/sonication (5 min) in 50 mmol/L Tris-HCl (pH 8.0) buffer containing 0.5 mol/L NaCl and 1 mmol/L phenylmethansulphonyl fluoride. The extracts were incubated at 60℃ for 30 min, and TF_1 β was purified using Ni^{2+}-NTA affinity chromatography at 4 ℃. The purified protein was analyzed by SDS-PAGE after dialysis and concentration.

The *R. rubrum* chromatophores and LiCl-treated chromatophores were prepared as referred to in refs. [12] and [13]. The Bchl content of chromatophores was determined at 880 nm using the *in vitro* extinction coefficient given by Clayton[14]. The reconstitution was carried out as described in refs. [12,13,15—17], and modified: reconsti-

tution buffer contained 50 mmol/L Tricine-NaOH(pH8.0), 4 mmol/L ATP, 25 mmol/L $MgCl_2$, 1 mmol/L dithiothreitol, 10% glycerol; 5 μg β-deleted chromatophores were reconstituted with 50 μg $TF_1β$. After incubation for 12 h at 37℃ the reconstituted system was centrifuged for 40 min at 22000×g. The pellet was resuspended in buffer containing 50 mmol/L Tricine-NaOH (pH 8.0), 10% glycerol and washed by the same buffer three times.

(iii) Activities assay of chromatophores. The ATP hydrolysis activity was measured as elucidated in ref. [18]. 1 μg reconstituted chromatophores were resuspended in 8 μL ATP synthesis buffer containing 50 mmol/L Tricine-NaOH(pH 8.0), 5 mmol/L $MgCl_2$, 4 mmol/L NaH_2PO_4, 15 mmol/L glucose, 5 mmol/L dithiothreitol. After adding 2 μL 10 mmol/L ADP, the chromatophores were illuminated for a prescribed time. By adding 1/10 volume of 4% TCA into it, the reaction stopped. To assay the ATP synthesis activity, the mixture was diluted with 20 volumes of buffer containing 100 mmol/L Tricine-acetate (pH 7.75), 2 mmol/L EDTA. The ATP yields were determined by luciferin/luciferase system.

(iv) Preparation of florescent actin filaments. FITC-labelled G-actin was obtained when the purified G-actin[19] was labeled with FITC for 30 min at 4℃ and the free FITC was removed from by dialysis. Then the FITC-labelled G-actin was polymerized in the buffer containing 50 mmol/L Hepes-KOH(pH7.6), 50 mmol/L KCl, 4 mmol/L $MgCl_2$, and 2 mmol/L ATP.

(v) Preparation of the rotation system. The actin filaments were treated with a 4—9 molar excess of Maleimido-C_3-NTA-Ni^{2+} in buffer A (50 mmol/L Hepes-KOH, pH7.6, 50 mmol/L KCl, 4 mmol/L $MgCl_2$) overnight at 4℃. The treated actin filaments were added to the hybrid chromatophores pellets and reacted for 30 min at room temperature. The unattached filaments were washed away by centrifuging.

(vi) Rotation assay. Fig. 1 shows the experimental system for the observation. The chromatophores obtained in "Materials and methods (v)" were introduced into the flow cell, where the glass surface was covered with polylysine. After being washed with buffer A 3—5 times, buffer B(50 mmol/L Tricine-NaOH, pH8.0, 5 mmol/L $MgCl_2$, 4 mmol/L Na_2HPO_4, 25 mmol/L glucose, 5 mmol/L dithiothreitol, 216 μg/mL glucose oxidase, 36 μg/mL catalase, 1% β-mercaptoethanol, 5 mmol/L NaN_3) was infused into the flow cell, and then it was covered with coverglass. After illumination for 30—60 min, the rotating actin filaments were observed and recorded immediately with an OlympusIX71 fluorescent microscope equipped with a CCD camera.

2 Results and discussion

(i) Restored ATP hydrolysis activity of the hybrid chromatophores. The chromatophores obtained by extraction of β subunit of F_1 with LiCl lose a majority of their ATP hydrolysis activity, but their capacity to take up protons is mostly retained[15]. Therefore, the chromatophores are proved to be convenient for investigation of the proton-conducting properties of F_oF_1-ATP synthase. Fig. 2 shows the SDS-PAGE of the purified $TF_1β_{10×His-tag}$. Fig. 3 plots the ATP hydrolysis activity restored by reconstitution from β-less chromatophores with purified $β_{10×His-tag}$ versus the incubation time. After 1-h incubation, 2.5% of ATP hydrolysis activity was restored. After incubation for 2 h, 13.6% of ATP hydrolysis activity was restored. After incubation for 4 h, it would be saturated. In order to get the maximal restored activity, the reconstitution was carried out by incubation for 12 h and about 40% of ATP hydrolysis activity was restored. However, in the previous studies of hybrid chromatophores, reconstitution with a variety of β subunits for 1-h incubation could restore over 40% ATP hydrolysis activity[15—17]. This is due to the different types of the β subunits.

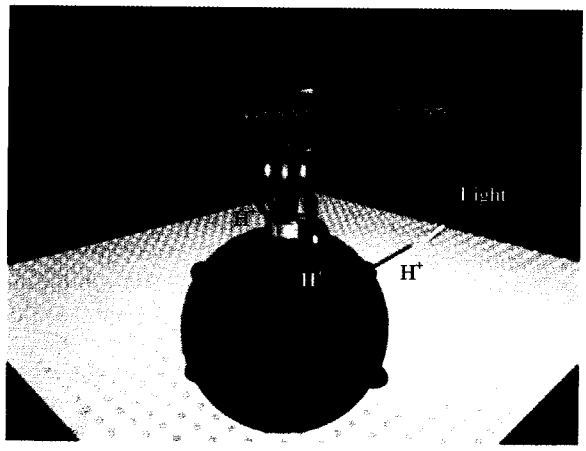

Fig. 1. The direct observation of β rotation in F_oF_1-ATP synthase motor. Experimental system for observing the clockwise rotation of fluorescent actin filaments connected to $β_{10×His-tag}$ of chromatophores-embeded F_oF_1 ATP synthase (δ-deleted) driven by light.

Fig. 4 shows the effects of specific inhibitors of F_oF_1-ATP synthase on the ATP hydrolysis activity of chromatophores. Both NaN_3 and efrapeptin are the specific inhibitors of F_1. Fig. 4(a) shows that the ATP hydrolysis activity of both coupled chromatophores and reconstituted chromatophores could be inhibited by 5 mmol/L NaN_3(46.9±2.8% and 56.1±0.7%, respectively). With the increasing concentration of NaN_3, the inhibition aggravated (data are not given). The coupled chromatophores and reconstituted chromatophores also showed good sensitivity to 1 mg/mL efrapeptin inhibition (53.7±4.0% and 69.0±2.2%, respectively). Fig. 4(b) shows the effects of two specific inhibitors of F_o on the ATP synthesis activity of chromatophores. It is well known that

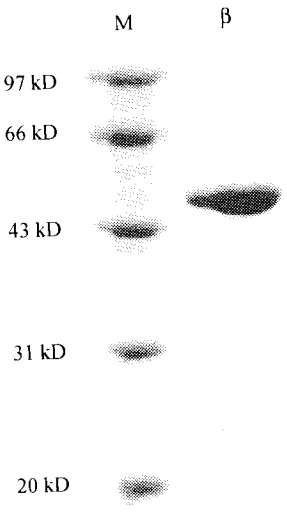

Fig. 2. The SDS-PAGE(13.5%) of purified $TF_1\beta$. M, Molecular weight marker; β, purified $TF_1\beta$.

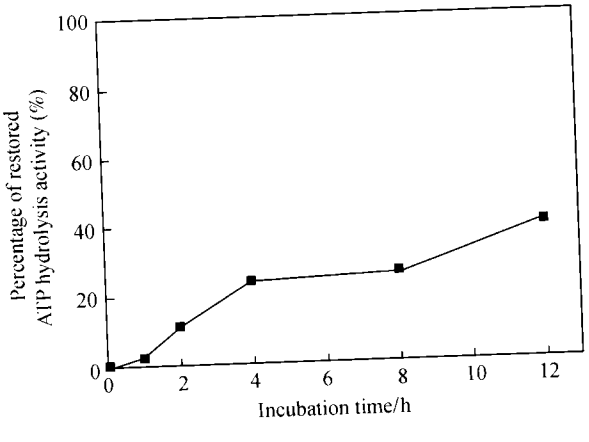

Fig. 3. The relationship between the incubation time and the ATP hydrolysis activity restored of reconstituted chromatophores. 5 μg β-less chromatophores and 50 μg $TF_1\beta$ were reconstituted at 37℃ and the ATP hydrolysis activity was assayed using "Materials and methods".

Oligomycin and DCCD are specific inhibitors of F_o. The coupled chromatophores and reconstituted chromatophores could be inhibited 69.4±1.5% and 15.4±3.1% by 2 mmol/L DCCD, respectively. Reconstituted chromatophores were insensitive to the inhibition of 20 μg/mL Oligomycin (3.2±0.4%), while coupled chromatophores were sensitive to it (49.2±3.1% inhibition). The above data indicate that the ATP hydrolysis activity of the hybrid chromatophores is presented by the reconstituted F_oF_1-ATP synthases.

(ii) Photophosphorylation of the hybrid chromatophores. Fig. 5 shows the photophosphorylation of hybrid chromatophores versus the time of illumination. Curve 2

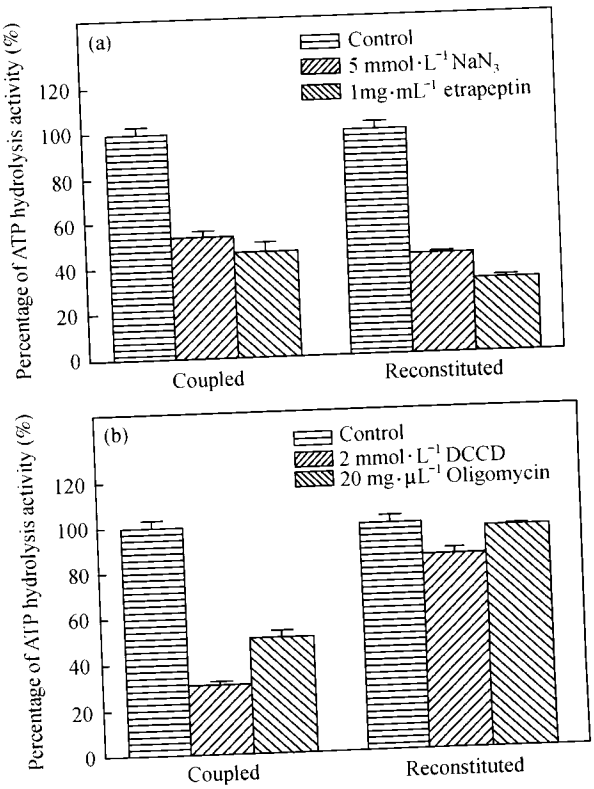

Fig. 4. The effects of specific inhibitors of F_oF_1-ATP synthase on the ATP hydrolysis activity of chromatophores. (a) The effects of specific inhibitors of F_1 on the ATP hydrolysis activity of chromatophores. 5 mmol/L NaN_3 was directly added into assay buffer; 1 mg/mL efrapeptin was preincubated with chromatophores for 10 min at 35℃. (b) The data were from two independent experiments. The effects of specific inhibitors of F_o on the ATP hydrolysis activity of chromatophores. 2 mmol/L DCCD and 20 μg/mL Oligomycin were preincubated with chromatophores for 10 min at 35℃, respectively.

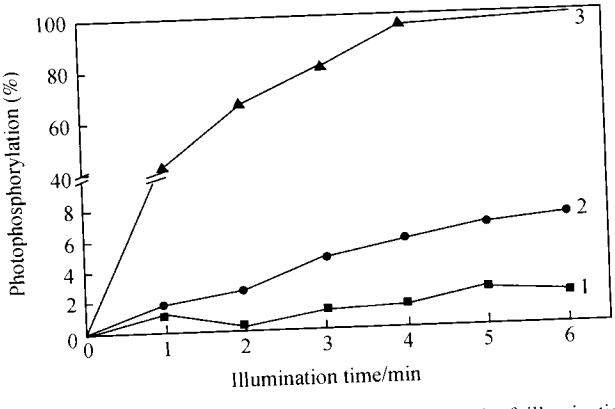

Fig. 5. The ATP synthesis following a short period of illumination monitored by luciferase/luciferin system in the chromatophores. 1 μg of β-less chromatophores (curve 1), reconstituted chromatophores (curve 2) and coupled chromatophores (curve 3) were illuminated under same conditions in varied time. The ATP yields were determined by the luciferase/luciferin system. The ATP yield of coupled chromatophores after 6-min illumination was designated as 100%.

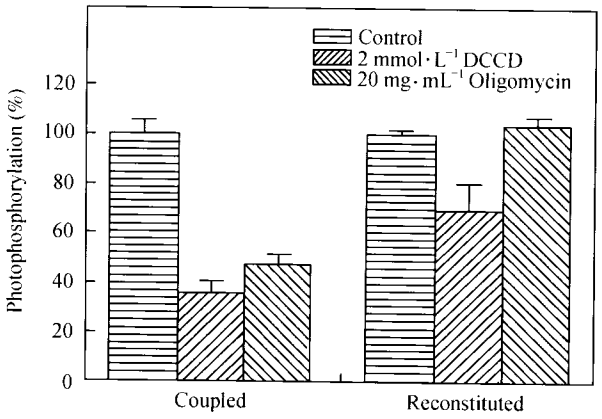

Fig. 6. The effects of specific inhibitors of F_o on the ATP synthesis activity of chromatophores monitored by luciferase/luciferin system. 2 mmol/L DCCD and 20 μg/mL Oligomycin were preincubated with chromatophores for 10 min at 35℃, respectively. The ATP yields were obtained after illumination for 5 min. The data were from three independent experiments.

shows that the ATP yield of reconstituted chromatophores increased from 0 to 7% after 6-min illumination, which is 3.7 times more than that of unreconstituted chromatophores (curve 1). Curve 3 shows that the ATP yields of coupled chromatophores increased from 0 to 100% (relative unit) after 6-min illumination.

As shown in Fig. 6, the ATP synthesis activity of reconstituted chromatophores was inhibited 30.6%±11.3% by 2 mmol/L DCCD. It is not sensitive to 20 μg/mL Oligomycin. This result is consistent with the sensitivity of the ATP hydrolysis activity to Oligomycin, while the ATP synthesis activity of coupled chromatophores is sensitive to not only 2 mmol/L DCCD (inhibited 63.9%±4.3%), but also 20 μg/mL Oligomycin (inhibited 52.5%±4.1%).

Many studies indicate that LiCl-treated *R. rubrum* chromatophores lose not only a majority of β subunit, but also a minority of α subunit[16]. Therefore, some of the δ subunits are lost in the chromatophores at the same time. In our experiment the restoration ratio of ATP synthesis activity (7%) was much lower than that of ATP hydrolysis activity (40%), because some of the reconstituted chromatophores lost δ subunit, causing their lower photophosphorylation[4].

The biochemical data indicate that the hybrid chromatophores have three properties:

(1) the capacity of transporting protons; (2) β subunit with a 10×His-tag ; (3) loss of δ subunit in some of them. The model for F_oF_1-ATP synthase of reconstituted chromatophores is shown in Fig. 7.

(iii) Observation of light-driven rotation within F_oF_1-ATP synthase. Fig. 8 shows the direct observation of clockwise rotation of F_oF_1-ATP synthase driven by light. The hybrid chromatophores labeled with fluorescent actin filaments were immobilized on glass surface. After illumination for about 30 min, the flow cell was observed under a fluorescent microscope. Fig. 8(a) shows the rotation of five fluorescent actin filaments (rotary rate, 1.2 revolution per second). Fig. 8(b) shows the sequential images of a fluorescent actin filament of L2, whose rotational direction is clockwise viewed from F_o side to F_1 (time interval between images, 30 ms). Fig. 8(c) shows the rotary angle of actin filament of L2 during a 10-s rotation. Fig. 8 also shows that the rotary rate is not constant because some of them have the occasional pause and backwardness, which are similar to the rotation of F_1 in previous reports[6–9]. The lengths of filaments, L1, L2, ···, L5 are 1.14, 1.25, 1.25, 1.21 and 2.00 μm respectively and the

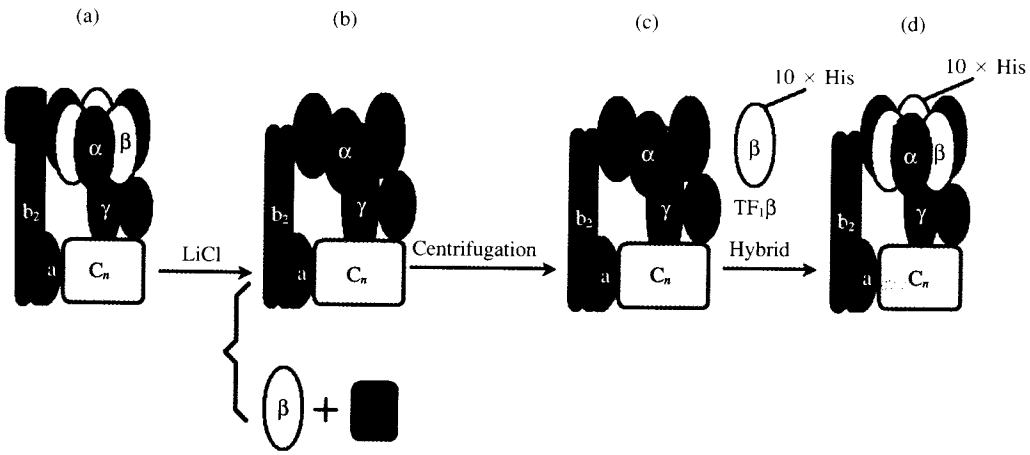

Fig. 7. Model of hybrid chromatophores used for single-molecule observation in our experiment. (a) F_oF_1-ATP synthase of coupled chromatophores; (b) F_oF_1-ATP synthase of LiCl-treatment chromatophores losing ATPase activities (F_1 depleted a lot of β subunit); (c) β, δ-depleted F_oF_1-ATP synthase obtained by centrifuging; (d) hybrid F_oF_1-ATP synthase reconstituted from $TF_1β$ and β, δ -depleted F_oF_1-ATP synthase.

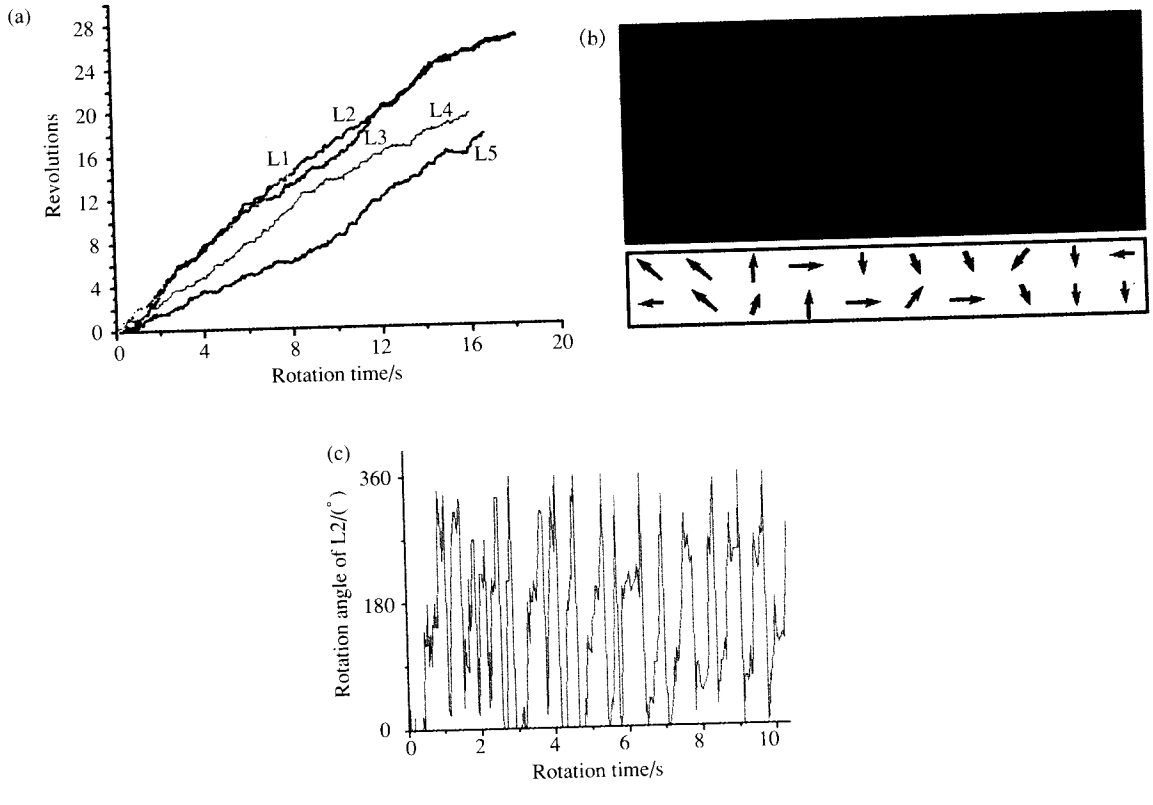

Fig. 8. The rotation of fluorescent actin filaments connected to the $\beta_{10\times His\text{-}tag}$ of hybrid F_oF_1-ATP synthase observed by a microscopy. (a) The relationship between the revolutions of fluorescent actin filaments and time courses. The lengths of fluorescent actin filaments, L1, L2, ···, L5 are 1.14, 1.25, 1.25, 1.21, 2.00 μm respectively, and the frictional torque for the filaments rotation is 5.63 pN • nm on average as calculated by $(2n\pi^2/3)\eta L^3/[\ln(L/2r)-0.447]$, where n is the rotary rate; $\eta(10^{-3}$ N • s • $m^{-2})$ is the viscosity of the medium; L is the length of actins filament; r (5 nm) is the radius of filament. Rotary rate, 1.2 revolution per second. (b) The sequential images of a rotating fluorescent actin filament of L2. Time interval between images, 30 ms; rotational orientation, clockwise viewed from the membrane side. (c) Rotational angle of the fluorescent actin filament of L2.

frictional torque for the filaments rotation is 5.63 pN • nm on average as calculated by $(2n\pi^2/3)\eta L^3/[\ln(L/2r)-0.447]$, where n is the rotary rate, $\eta(10^{-3}$N •s •$m^{-2})$ is the viscosity of the medium, L is the length of actins filament, and r (5 nm) is the radius of filament[20].

3 Conclusion

It is clearly known that F_oF_1-ATP synthase is a rotary motor and can be functionally divided into two parts: stator and rotor. The former is composed of the $\alpha_3\beta_3\delta$ sub-complex belonging to F_1 and ab_2 sub-complex of F_o. The latter is composed of $\varepsilon\gamma$ sub-complex and C_n sub-complex. The studies *in vitro* indicate that the stator and rotor are reversible during ATP hydrolysis or synthesis. When the $\alpha_3\beta_3\delta ab_2$ complex is immobilized, $\varepsilon\gamma C_n$ is rotor, when $\varepsilon\gamma C_n$ is immobilized, $\alpha_3\beta_3\delta ab_2$ becomes rotor.

Figure 7 is a model of hybrid chromatophores used for single-molecule observation in our experiment. Fig. 7(a) is the F_oF_1-ATP synthase of coupled chromatophores; Fig. 7(b) is the F_oF_1-ATP synthase of LiCl-treatment chromatophores losing ATPase activities (F_1 is depleted of β subunit and some of δ subunit) and Fig. 7(c) plots the β, δ-depleted F_oF_1-ATP synthase obtained by centrifuging; Fig. 7(d) is the hybrid F_oF_1-ATP synthase reconstituted from $TF_1\beta$ and β, δ-depleted F_oF_1-ATP synthase.

It is the first time that clockwise rotation of the F_oF_1-ATP syntheses was observed directly to be driven by light when viewed from the F_o side to F_1. Therefore, further optimization and development of the hybrid chromatophores will make it an important system for investigation of the coupling property of F_oF_1-ATP synthase.

Acknowledgements We thank Profs. Yang Fuyu, Zhou Junmei and Li Shengguang for their helpful discussion and encouragements. We also thank Miss Liu Li for drawing the picture of Fig. 1 and Dr. Ren Quan in Institute of Mechanics, CAS, for his reading the manuscript. This work was supported by the National Natural Science Foundation of China (Grant Nos. 30240042, 30292905, 90306005 and 19890384-4).

References

1. Capaldi, R. A., Schulenberg, B., Murray, J. et al., Cross-linking and electron microscopy studies of the structure and functioning of the *E. coli* ATP synthase, J. Exp. Biol., 2000, 203(1): 29—33.
2. Stock, D., Gibbons, C., Arechaga, I. et al., The rotary mechanism of ATP synthase, Current Opinion in Structural Biology, 2000, 10: 672—679.

3. Senior, A. E., Nadanaciva, S., Weber, J., The molecular mechanism of ATP synthesis by F_1F_o-ATP synthase, Biochimica et Biophysica Acta, 2002, 1553: 188—211.
4. Weber, J., Wilke-Mounts, S., Senior, A. E., Quantitative determination of binding affinity of δ-subunit in *E. coli* F_1-ATPase, J. Biol. Chem., 2002, 277 (21): 18390—18396.
5. Noji, H., Yasuda, R., Yoshida, M. et al., Direct observation of the rotation of F_1-ATPase, Nature, 1997, 386(20): 299—302.
6. Noji, H., Yoshida, M., The rotary machine in the cell, ATP synthase, J. Biol. Chem., 2001, 276(3): 1665—1668.
7. Yasuda, R., Noji, H., Yoshida, M. et al., Resolution of distinct rotational substeps by submillisecond kinetic analysis of F_1-ATPase, Nature, 2001, 410: 898—904.
8. Hirono-Hara, Y., Noji, H., Nishiura, M. et al., Pause and rotation of F_1-ATPase during catalysis, Proc. Natl. Acad. Sci. USA, 2001, 98(24): 13649—13654.
9. Yasuda, R., Noji, H., Kinosita, K. J. et al., F_1-ATPase is a highly efficient molecular motor that rotates with discrete 120° steps, Cell, 1998, 93: 1117—1124.
10. Adachi, K., Yasuda, R., Noji, H. et al., Stepping rotation of F_1-ATPase visualized through angle-resolved single-fluorophore imaging, Proc. Natl. Acad. Sci. USA, 2000, 97(13): 7243—7247.
11. Montemagno, C., Bachand, G., Constructing nanomechanical devices powered by biomolecular motors, Nanotechnology, 1999, 10: 225—231.
12. Gromet-Elhanan, Z., Khananhvili, D., Methods Enzymol., 1986, 126: 528—538.
13. Philosoph, S., Binder, A., Gromet-Elhanan, Z., Coupling factor ATPase complex of *Rhodosspirillum rubrum*, J. Biol. Chem., 1977, 252(23): 8747—8752.
14. Clayton, R. K., Absorption spectra of photosynthetic bacteria and their chlorophylls, Bacterial Photosynthesis (eds. Gest, H., Pietro, A. S., Vernon, L. P.) OH: Antioch Press, 1963, 495—500.
15. Gromet-Elhanan, Z., Daniel, K., Sara, W. et al., ATP synthesis and hydrolysis by a hybrid system reconstituted from the β-subunit of *E. coli* F_1-ATPase and β-less chromatophores of *Rhodospirillum rubrum*, J. Biol. Chem., 1985, 260(23): 12635—12640.
16. Ward, C. T., Du, Z. Y., Hein, R. et al., Hybrid *Rhodospirillum rubrum* F_oF_1ATP synthases containing spinach chloroplast $F_1\beta$ or α and β subunits reveal the essential role of the α subunit in ATP synthesis and tentoxin sensitivity, J. Biol. Chem., 2000, 275(2): 906—912.
17. Gromet-Elhanan, Z., The proton-translocating F_oF_1ATP synthase-ATPase complex, Anoxygenic Photosynthetic Bacteria (eds. Blankenship, R. E., Madigan, M. T., Bauer, C. E.), The Netherlands: Kluwer Academic Publishers, 1995, 807—830.
18. Matsui, T., Yoshida, M., Expression of the wild-type and the Cys-/Trp-less $\alpha_3\beta_3\gamma$ complex of thermophilic F_1-ATPase in *E. coli*, Biochima. Biophys. Acta, 1995, 1231(2): 139—146.
19. Spudich, J. A., Watt, S., The regulation of rabbit skeletal muscle contraction, J. Biol. Chem., 246(15): 4866—4871.
20. Wang, X. S., Cui, Y. B., Zhang, Y. H. et al., Direct observation on single molecular rotation of high activity F_1-ATPase, Prog. Biochem. Biophys. (in Chinese), 2003, 30(2): 194—198.

(Received January 7, 2004; accepted April 25, 2004)

Chinese Science Bulletin 2004 Vol. 49 No. 13 1347—1353

Pedigree transmission disequilibrium test for QTL mapping of threshold trait

DING Xiangdong, ZHANG Qin, XU Ruhai & WANG Yachun

The Key Laboratory of Animal Genetics and Breeding of the Ministry of Agriculture, Beijing 100094; State Key Laboratory for Agrobiotechnology, Beijing 100094, China
Correspondence should be addressed to Zhang Qin (e-mail: qzhang@cau.edu.cn)

Abstract **With biological and economic importance, threshold traits are discrete in phenotype but have the same polygenic genetic basis as quantitative traits. The traditional linkage analysis for quantitative traits is invalid for threshold traits due to their special characters. The transmission disequilibrium test (TDT) has received great attention recently in localizing human disease genes due to its simplicity and powerfulness. But TDT only deals with data from independent nuclear families and it will lose information about extended pedigree that incorporates information not only from parents and siblings but also from other relatives. The pedigree disequilibrium test (PDT) proposed by Martin in 2001 can be used to analyze the extended pedigree in human. In this study, PDT was introduced into the QTL mapping of threshold traits for farm animals, and was modified in order to accommodate the pedigree structures of farm animals. The modified PDT was renamed pedigree transmission disequilibrium test (PTDT) and its power and type I error were investigated and compared with that of PDT by Monte Carlo simulation. It was shown that PTDT is a robust and valid approach to mapping QTL of threshold trait. When the parental information is complete, PTDT and PDT are almost the same in terms of power and type I error. However, if the parental information is missing to a certain extent, PTDT is higher in power and lower in type I error than PDT. These results imply that PTDT can be a novel approach to QTL fine mapping of threshold traits based on the existing coarse mapping information.**

Keywords: threshold trait, QTL mapping, pedigree transmission disequilibrium test, extended pedigree.

DOI: 10.1360/04wc0050

Threshold traits are discrete in phenotype but not inherited in a simple Mendelian fashion. They are controlled by polygenes like quantitative traits. The great development in genomics makes it possible to unveil the genetic basis of threshold trait from molecular level. QTL can be mapped and its effect can be estimated using the segregation information of markers linked with QTL. QTL mapping using markers has been a research hotspot since it was proposed in 1961. However, there are only few researches having been done on QTL mapping for threshold traits. In farm animals, many threshold traits, such as dis-

ease resistance and litter size of monotocous species, are of biological and economic importance. The linkage analysis has been proved to be a successful method for QTL mapping for continuous quantitative traits in farm animals; however, it is invalid for threshold traits due to their special characteristics.

Identifying disease genes is the main task in the field of human gene mapping. The genetic mechanisms of many diseases, which are often referred to as complex traits in human genetics, are similar to those of threshold traits. The transmission disequilibrium test (TDT) was first proposed by Spielman et al.[1] for mapping genes responsible for disease resistance. The basic idea behind TDT is to compare the frequency at which an allele of interest is transmitted from heterozygous parents to affected offspring with the frequency at which other alleles are transmitted from these same heterozygous parents to affected offspring. TDT has aroused great attention recently in localizing human disease genes due to its simplicity and powerfulness and become the core of family based association study. TDT has been extended to deal with families with multiple affected offspring, discordant sibship, and families with only one parent available[2–8]. It was shown that TDT is more powerful than linkage analysis when markers are tightly linked with QTL[9,10].

Extended pedigree is popular in human and animals and rich in information. It incorporates information not only from parents and siblings but also from other relatives. But the original TDT and its extensions are not valid test of association for extended pedigrees; moreover, they may waste a lot of information. It would be desirable to extend TDT to deal with extended pedigrees including all potentially information. The pedigree disequilibrium test (PDT) proposed by Martin[11,12] is able to analyze extended pedigrees in human. Extended pedigrees are more common, more informative, more valuable, and easier to obtain in farm animals than in human beings. So, introducing PDT into farm animals for threshold trait analysis is the first objective of this study. Usually, there are much more offspring per family in some species of farm animals than in human, and the proportion of affected offspring is low. As the traditional TDT method, PDT ignores the transmission information of the unaffected offspring. Considering this special feature of farm animals, the second objective of this study is to develop a novel approach to QTL mapping of threshold traits using the transmission information of both affected and unaffected offspring based on PDT. We named the modified PDT pedigree transmission disequilibrium test (PTDT).

1 Methods

(i) Pedigree transmission disequilibrium test (PTDT). Assume that a nuclear family consists of both parent and at least one child. Several related nuclear families make up an extended pedigree. And a threshold trait has two categories, namely status 1 (it can be understood as affected in the case of disease trait) and status 2 (or unaffected). There are two types of nuclear families that may provide information on linkage disequilibrium: (1) family with at least one status 1 offspring, both parents available, and at least one parent is heterozygous at the marker being studied; (2) family with at least one discordant sibship and the parental information may or may not available. A discordant sibship is defined as a pair of siblings, who are different in phenotypic status and in marker genotypes. An extended pedigree will be considered informative if it contains at least one nuclear family of either type.

For an extended pedigree, let n_T and n_S denote the number of the first and second type nuclear families, respectively. Consider a marker locus with two alleles, M_1 and M_2. For the first type nuclear families, let N_{ta} and N_{tu} be the times the heterozygous parents transmit M_1 to their status 1 and status 2 offspring, respectively, N_{na} and N_{nu} be the times the heterozygous parents do not transmit M_1 to their status 1 and status 2 offspring, respectively. A random variable X_T is defined as

$$X_T = (1-u)(N_{ta} - N_{na}) - u(N_{tu} - N_{nu}),$$

where u is the prevalence proportion of status 1 in the population. In Martin's PDT[11], X_T was defined as $N_{ta} - N_{na}$, i.e. it ignores the transmission information of the status 2 offspring. Since both status 1 and status 2 offspring provide transmission information, PTDT might improve the power by considering the additional transmission information from status 2 offspring, especially for the threshold trait with high prevalence of status 1[13].

For the second type of nuclear families, let N_{sa} and N_{su} denote the number of M_1 in status 1 and status 2 offspring of a discordant sibship. A random variable X_S is defined as

$$X_S = N_{sa} - N_{su}.$$

For an extended pedigree, a summary random variable D is defined as

$$D = \frac{1}{n_T + n_S}\left(\sum_{j=1}^{n_T} X_{T_j} + \sum_{j=1}^{n_S} X_{S_j}\right).$$

Under the null hypothesis of no linkage disequilibrium between the marker and QTL, $E(X_T) = 0$ for all first type of nuclear families and $E(X_S) = 0$ for all second type of nuclear families. Consequently, $E(D) = 0$ for any extended pedigree. For N independent extended pedigrees, under the null hypothesis,

$$E\left(\sum_{i=1}^{N} D_i\right) = 0,$$

$$\mathrm{Var}\left(\sum_{i=1}^{N} D_i\right) = \sum_{i=1}^{N} \mathrm{Var}(D_i) = E\left(\sum_{i=1}^{N} D_i^2\right),$$

where N is the number of extended pedigrees. Hence, we